



PhD Thesis

PhD Thesis

PhD Thesis
by Niclas Lars Rudolf Fiedler, M.Sc.
from Weilmünster
XX.XX.2028

Justus Liebig University Gießen
Institute of Experimental Physics II

First Examiner: Prof. Dr. Kai-Thomas Brinkmann
Second Examiner: Prof. Dr. Jens Sören Lange, AkR
Supervisor: Dr. Dzmitry Kazlou

Abstract

Zusammenfassung

Contents

Abstract	iii
Zusammenfassung	iv
1 Detector Design and Construction	1
1.1 Introduction & Motivation	1
1.2 Detector Concept & Scintillator Selection	1
1.3 Detector Simulation	2
1.3.1 Detector Implementation	2
1.4 Readout	3
1.5 Detector Housing	4
1.5.1 Wrapping	4
1.5.2 Light Yield Measurement	5
1.5.2.1 Light Yield: PbWO ₄	5
1.5.2.2 Light Yield: EJ-200	7
1.6 Photon Readout and SiPM Selection	9
1.6.1 SiPM for PbWO ₄	9
1.6.2 SiPM for EJ-212	11
1.7 Detector Assembly and Construction	12
1.8 Experimental Setup	12

1.9 Data Analysis	12
1.10 Results	12
1.11 Discussion	12
1.12 Outlook	12

Bibliography**I****List of Figures****II****List of Tables****III**

Chapter 1

Detector Design and Construction

1.1 Introduction & Motivation

1.2 Detector Concept & Scintillator Selection

Two different scintillation-based detector-concepts were developed to measure the depth dose distribution of protons in real-time. Both detectors consist of 32 scintillator-layers read-out via **Silicon PhotoMultipliers (SiPMs)** and two linked-together 16-channel CAEN digitizer.

The first detector concept is PbWO₄-based, as the first prototype, [citemaster], but improves on the layer geometry by using sheets instead of bars whilst also reducing layer thickness. For this two crystal sizes were chosen with $30 \times 30 \times 3 \text{ mm}^3$ and $30 \times 30 \times 2 \text{ mm}^3$, which were provided and cut by Crytur, allowing full coverage of the 220 MeV proton range of $\approx 66 \text{ mm}$. The lateral sheet sizes with 30 mm were the largest provided, because the sheets were cut from a single ingot and the thicknesses are the smallest resonable due to PbWO₄ being very fragile. The 3 mm thick sheets are used in the front or shallow beam depths to provide more stopping power and the thinner 2 mm sheets are used in the Bragg-Peak region to give an optimal spatial resolution.

The second detector concept using plastic scintillators was developed to further increase the spatial resolution in the Bragg-Peak region at the cost of dynamic range in the shallow depths. Plastic scintillators were chosen because they have a much lower density and

thereby stopping power than PbWO₄ and a high light yield also giving a better energy resolution. However, to achieve a high spatial resolution whilst using only 32 channels, individual channels need a low radiological thickness resulting in not fully covering the proton range. To still stop the proton beam, a passive absorber with a known stopping power i.e. radiological thickness is incorporated between the first and second scintillator layers. This allows the first to work as a trigger channel which is used for the normalization in the analysis.

1.3 Detector Simulation

Geant4 simulations of both detector designs were implemented to give insights into their respective performances and to strike a good balance between active and passive volume for the plastic based detector. For this the reference physics list QGSP_BIC_EMY was chosen with the addition of substituting G4EmStandardPhysics_option3 with G4EmStandardPhysics_option4. The production cut was uniformly set to 0.05 mm for all particle types, which corresponds to an energy threshold of approximately 55 keV for electrons in water [[<empty citation>](#)](baumann2017). This threshold defines the minimum range a secondary particle must have to be explicitly generated in the simulation; particles with shorter ranges deposit their energy locally without being tracked as individual secondaries.

1.3.1 Detector Implementation

The PbWO₄-based detector was implemented as 32 PbWO₄ sheets with the dimensions from Section 1.2. The mean excitation energy was set to 600.7 eV(citation needed), Birks' Coefficient to 0.008694 $\frac{\text{MeV}}{\text{cm}}$, the absorption length to 100 cm, the lightyield to 200 ph/MeV and the refractive index to 2.2 (citation). The crystals are wrapped in 0.25 mm PTFE-foil and 20 μm aluminum foil per side, as measured in Section ??(reference needed). Here PTFE is modeled after its molecular formula of the repeating unit C₂F₄ with a density of $\rho_{\text{PTFE}} = 2.2 \frac{\text{g}}{\text{cm}^3}$ and a mean excitation energy of $I_{\text{PTFE}} = 99.1 \text{ eV}$ [citation needed] and the aluminum foil (99.9 %) is approximated by solid aluminum.

The plastic based detector was implemented using an active and passive material. The active material was modeled after a PVT-based scintillator, similar to general purpose plastic

scintillators like EJ-200 or BC-408. Here, the material is composed out of hydrogen and carbon with the mass fractions of 8.5 % and 91.5 %, respectively [citeEJ]. The passive material is PMMA and modeled after its molecular formula of the repeating unit $C_5H_8O_2$ with a density of $\rho_{PMMA} = 1.9 \frac{g}{cm^3}$ and a mean excitation energy of $I_{PMMA} = 74 \text{ eV}$ [citationneeded]. Here, the scintillators are again wrapped in PTFE and aluminum foil.

From Equation ?? follows that a 220 MeV proton beam has a range of 30.45 cm in water. Considering that plastic scintillators have a very similar stopping power and that the Bragg-Peak region is about 1/3 of the depth-dose distribution this leads to a scintillator thickness of $\approx 4 \text{ mm}$. For the 32 available channels this gives a coverage of $\approx 12.8 \text{ cm}$ of the 30.45 cm proton range, resulting in a $\approx 20 \text{ cm}$ passive absorber. To chose the right thickness of the PMMA absorber, its water equivalent radiological thickness after the first scintillator layer has to be calculated. This is done using the total energy deposition inside the absorber by integrating Equation ??(range energy), as shown in Equation 1.1.

$$\Delta E_{H_2O} = \Delta E_{mat} \quad (1.1)$$

$$\int_{z_n}^{z_{n+1}} S_{H_2O} dz = \int_{x_n}^{x_{n+1}} S_{mat} dx \quad (1.2)$$

$$E(z_{n+1})_{H_2O} - E(z_n)_{H_2O} = E(x_{n+1})_{mat} - E(x_n)_{mat} \quad (1.3)$$

$$E(z_n)_{H_2O} = E(x_n)_{mat} \rightarrow E(z_{n+1})_{H_2O} = E(x_{n+1})_{mat} \quad (1.4)$$

$$x_{n+1} = x_n + \Delta x \rightarrow \left(\frac{z_{n+1}}{\alpha_{H_2O}} \right)^{\frac{1}{p_{H_2O}}} = \left(\frac{x_n + \Delta x}{\alpha_{mat}} \right)^{\frac{1}{p_{mat}}} \quad (1.5)$$

$$x_n = \alpha_{mat} \left(\frac{z_n}{\alpha_{H_2O}} \right)^{\frac{p_{mat}}{p_{H_2O}}} \rightarrow z_{n+1} = \alpha_{H_2O} \left(\left(\frac{z_n}{\alpha_{H_2O}} \right)^{\frac{p_{mat}}{p_{H_2O}}} + \frac{\Delta x}{\alpha_{mat}} \right)^{\frac{p_{H_2O}}{p_{mat}}} \quad (1.6)$$

using $z_0 = x_0 = 0$.

1.4 Readout

The scintillators of both designs are read out via SiPMs. Light yield measurements were conducted, to decide which SiPM types are suitable. With these the amount of incident

photons can be estimated and compared with the number of pixel. From this, a balance can be struck between high resolution and a large enough dynamic range.

1.5 Detector Housing

The scintillators are held in place by a custom 3D-printed PLA housing, as shown in Figure ??(fig needed). The crystals are spaced 6.6 mm center-to-center, leaving 3 mm of space inbetween for calibration sources. Small crevices on the top side allow for easy insertions of sources using the custom 3D-printed tool shown in Figure ???. Spring blocks 3D-printed out of flexible TPU, shown in Figure ??, are used to lightly press the scintillators onto the SiPMs. The spring blocks are moved using screws and heat-set threaded inserts on the left. Markings indicate the correct beam alignment.

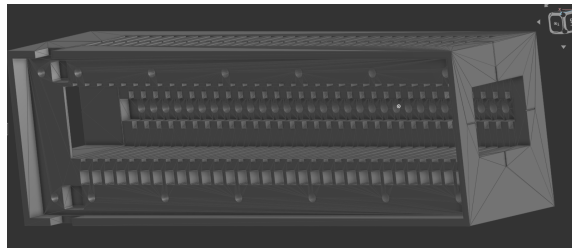
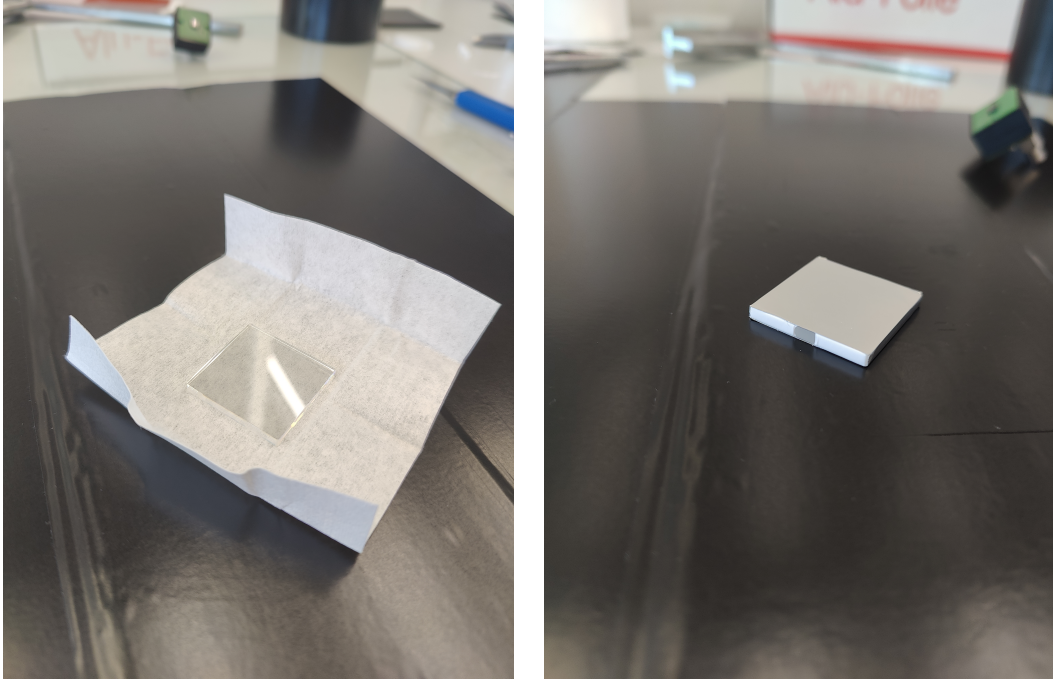


Figure 1.1: Caption

1.5.1 Wrapping

The crystals were wrapped in a high-reflectivity PTFE membrane to increase the light yield and decrease the cross-talk probability. For this the crystals are first cleaned with ethanol, as shown in Figure 1.2a. Then they are tightly wrapped in three layers of PTFE membrane, with an SiPM-sized window cut-out on one side where the SiPM will be attached, as shown in Figure 1.2a. The PTFE-membrane is the Tetratex® ePTFE-membrane with 127 μm membrane thickness at a density of 0.35 g/cm³ [1]. It reflects the scintillation light back inside the crystal so that it can only exit the crystal on the open side where the SiPM is located. The wrapped crystals are additionally wrapped tightly in one layer of 20 μm [1] aluminum foil, fixated using reflective tape, as shown in Figure 1.2b. This

protects the wrapping and ensures light-tightness from both inside and outside. Its reflectiveness helps redirect any remaining light that might pass through the PTFE, particularly on the edges and corners where the wrapping is thinnest.



(a) Cleaned PbWO₄ crystal.

(b) Fully wrapped PbWO₄ crystal with window cut-out.

1.5.2 Light Yield Measurement

The measurements were conducted using the process described in Section ?? and the setup shown in Figure ?? . The PMT used is an R2059 from Hamamatsu (serial number BA3200) with a quantum efficiency of 23.16 % [2] (cf. Appendix ??) at the luminescence peak of 420 nm of PbWO₄ [3] and EJ212.

1.5.2.1 Light Yield: PbWO₄

The PbWO₄ measurement were done in a flat and vertical position as shown in Figure 1.3, where all non PMT-facing scintillator sides were enveloped in highly reflective

PTFE foil in order to not lose any photons. Two additional measurements were performed, where one 3 mm- and 2 mm crystal were fully wrapped with an SiPM sized window cutout in the center of one side as shown in Figure ???. The PbWO₄ crystals were mounted onto the PMT's optical window next to a ²²Na γ -source inside a climate chamber. The optical coupling was done using glycerol ($n = 1.4722$), as shown in Figure ???. Glycerin was used as a substitute for the commonly used Baysilone® Fluid M optical grease ($n \approx 1.404$, $\eta = 300\,000\,\text{mm}^2/\text{s}$ [4]), due to its less-adhesive characteristic. The Baysilone® Fluid M with its high adhesion might have lead to damaging the fragile crystals during removal. The refractive index of PbWO₄ and the SiO₂ glass window of the PhotoMultiplier Tube (PMT) are $n_{\text{PbWO}_4} \approx 2.3$ [3] and $n_{\text{SiO}_2} \approx 1.459$ [5], respectively. Additionally to the climate chamber's light-tightness, the setup is enclosed in PTFE foil, ensuring perfect light tightness.

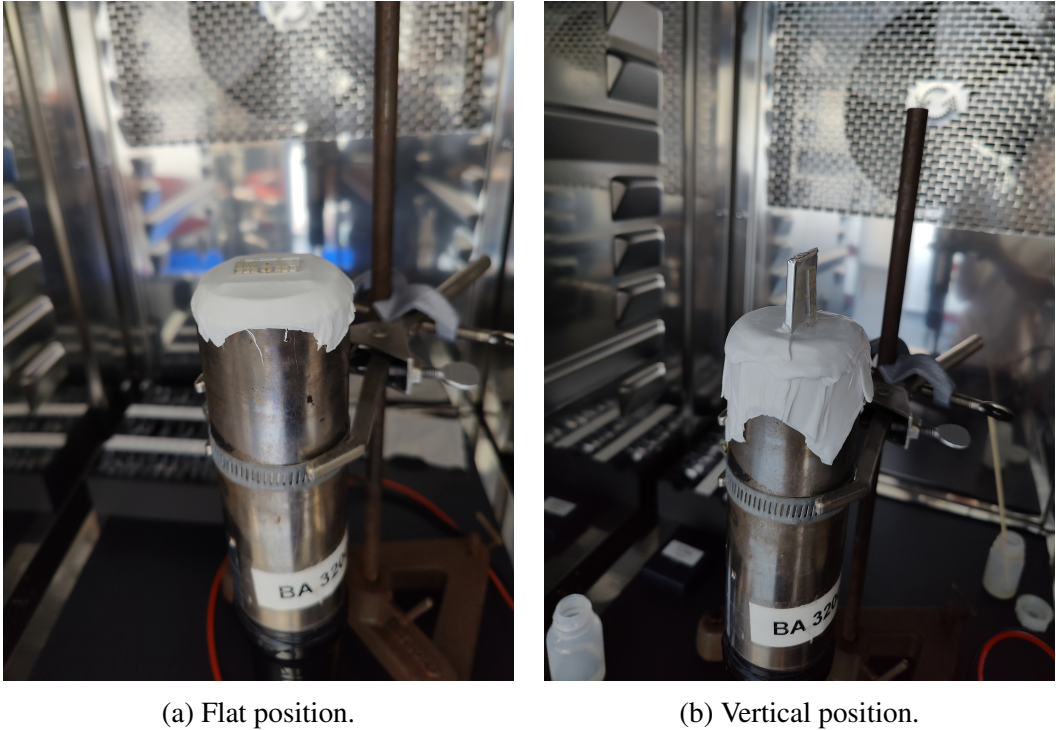


Figure 1.3: Measurement positions of the PbWO₄ scintillators on the PMT for the light yield measurements using a ²²Na source.

The measurements were conducted at 20 °C for 5 min after an acclimation time of 5 min each. The acclimation time was chosen small because the crystals were kept inside

the climate chamber for 24 h before the measurements were started, thereby only the short time frame in between measurements, where the chamber was opened, had to be accounted for. An exemplary light yield measurement of crystal number 0 in the flat position is shown in Figure 1.4. The measured light yield values of all crystals and their averages for the different setups are shown in Figure 1.5. The 3 mm thick crystals average approximately 164.73 ph/MeV and 129.44 ph/MeV in the flat and vertical positions, respectively. The 2 mm thick crystals average approximately 131.00 ph/MeV and 94.32 ph/MeV in the flat and vertical positions, respectively. With the SiPM-sized window cutout the light yield of a 3 mm and 2 mm crystal was (75.25 ± 33.09) ph/MeV and (59.70 ± 19.22) ph/MeV, respectively.

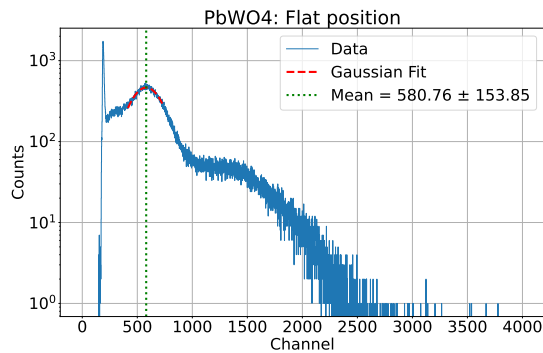


Figure 1.4: Example light yield measurement of the 3 mm thick PbWO₄-crystal number 0 in flat position on the PMT using a ²²Na source.

1.5.2.2 Light Yield: EJ-200

The light yield of a $50 \times 50 \times 10$ mm³ EJ-200 sample was measured to estimate the amount of incident photons on an SiPM optically coupled to an EJ-212 scintillator, which has similar properties to EJ-200, to decide which SiPM type is needed for the readout.

The measurements were done in a flat and vertical position, with two source positions for the vertical setup, as shown in Figure 1.6. In the vertical position two wrappings for the scintillator were used. First the whole PMT facing side was left open and secondly only an SiPM-sized window cutout was left open. The scintillator was mounted onto the PMT's optical window inside a climate chamber and optically coupled using Baysilone® Fluid M

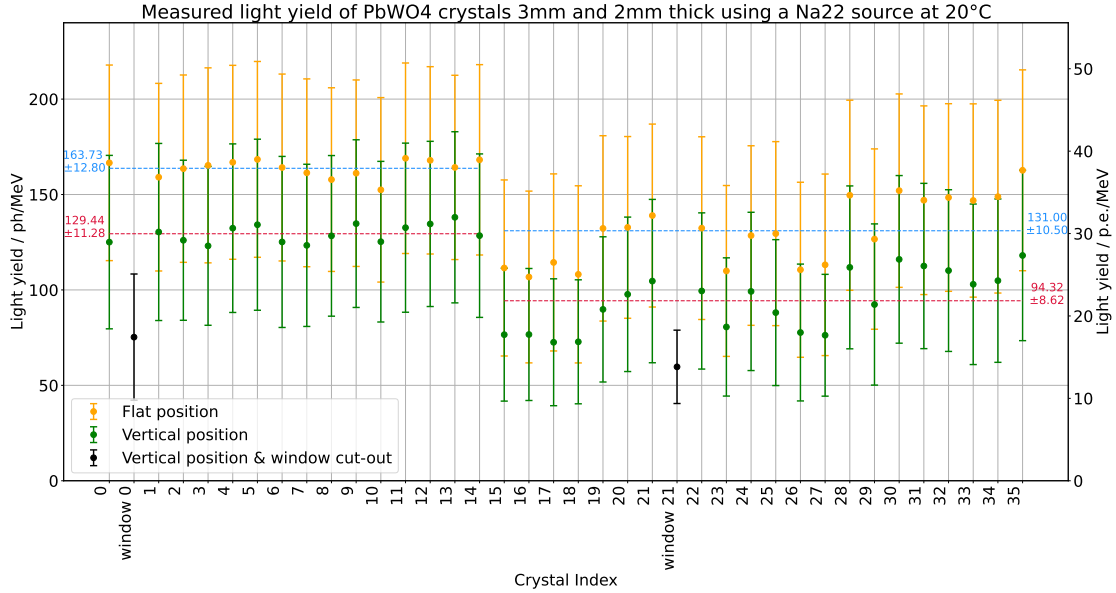


Figure 1.5: Light yield measurements of PbWO₄-crystals in flat and vertical positions including two window cut-out measurements using a ²²Na source.

optical grease [4]. The setups were fully enclosed in PTFE foil to ensure light-tightness. The source positions were on the side and on top of the scintillator. A ²⁴¹Am source was chosen due to the high light yield of EJ200 as ²⁴¹Am has a prominent low-energy gamma line at 59.6 eV.

The measurements were conducted at 20 °C for 20 min after an acclimation time of 24 h. The measurements and Gaussian fits of the 59.6 eV peak are shown in Figure 1.7.

The light yield results are shown in Table 1.1. The light yield for the flat position is in good agreement with the value provided by the manufacturer of 10 000 ph/MeV, taking into account aging-related degradation of the PMT (from 2012), which reduce the quantum efficiency. For both vertical positions, the light yield is only slightly affected by the source position. This is due to the high attenuation length of optical photons in the scintillator of 380 cm. When photons are collected from one side, approximately 30 % of the total light is lost and when using an SiPM-sized window cut-out the light yield is reduced by 70 %.

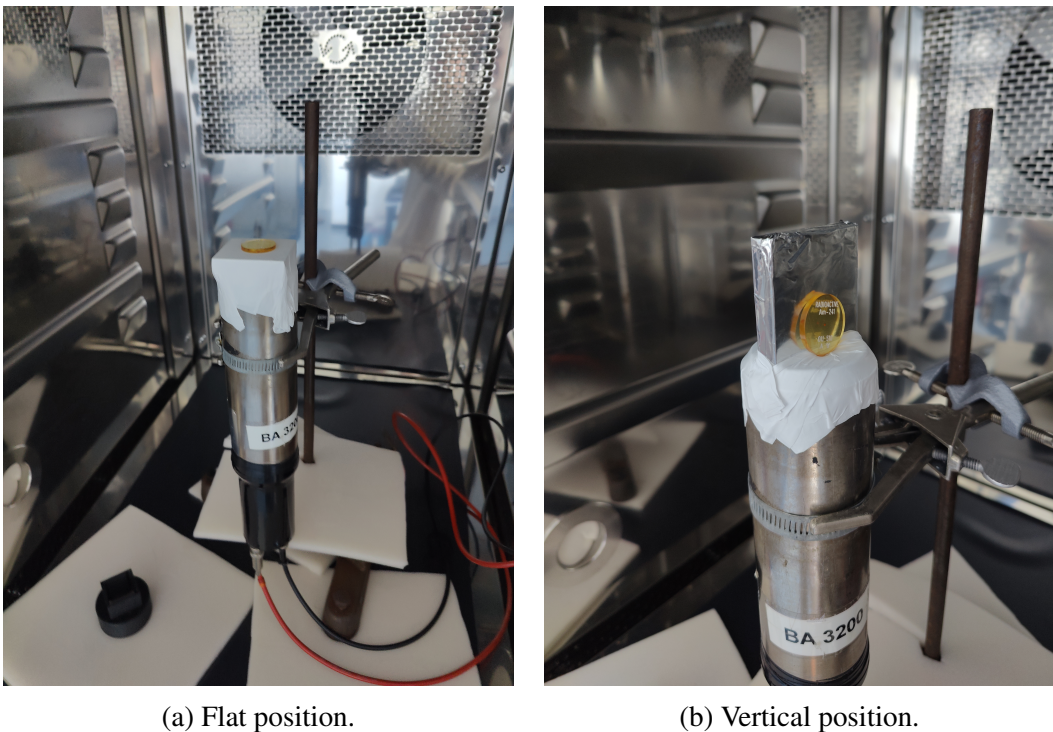


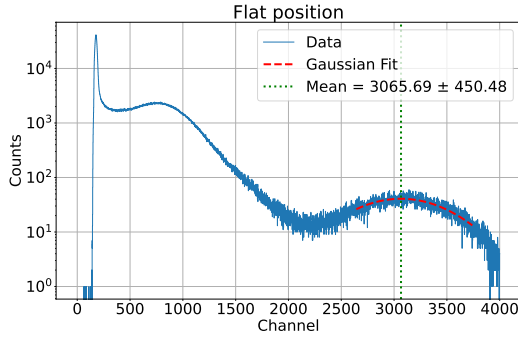
Figure 1.6: Measurement positions of the EJ-200 scintillator on the PMT for the light yield measurements using a ^{241}Am source.

1.6 Photon Readout and SiPM Selection

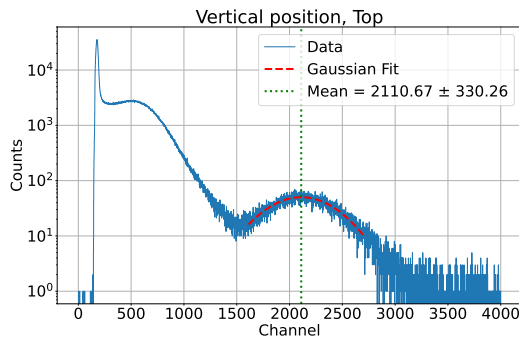
An optimal SiPM-type for measuring the proton depth-dose distribution for the given scintillators needs to balance a high resolution with a high dynamic range to accurately measure the low energies in the shallow depths and the high energies in the Bragg-Peak region. To ensure a linear SiPM signal, the number of impinging photons needs to be less or equal to approximately 10 % of the number of pixels divided by the Photo-Detection Efficiency (PDE).

1.6.1 SiPM for PbWO₄

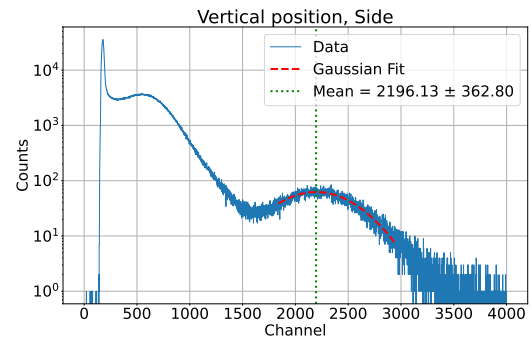
The light yield measurements of the teflon-wrapped PbWO₄ crystals with an SiPM-sized window cutout resulted in (75.25 ± 33.09) ph/MeV and (59.70 ± 19.22) ph/MeV for the



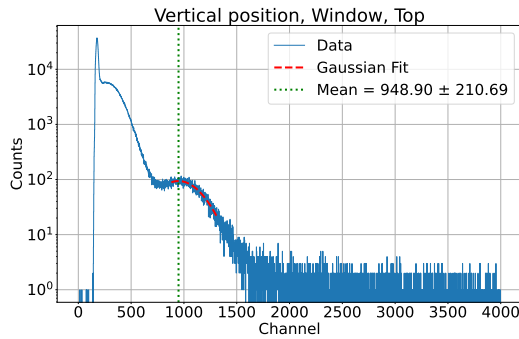
(a) Flat scintillator position.



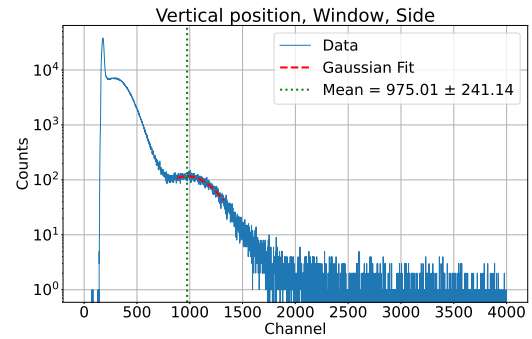
(b) Vertical position with open side and source on top.



(c) Vertical position with open side and source on the side.



(d) Vertical position with SiPM-sized window cutout and source on top.



(e) Vertical position with SiPM-sized window cutout and source on the side.

Figure 1.7: Light yield measurements of the $50 \times 50 \times 10\text{mm}^3$ EJ-200 scintillator sample. Shown are the measurements of the scintillator in a flat position with a completely open side (1.7a), in a vertical position with open side and the source on top (1.7b) and on the side (1.7c), and in a vertical position with an SiPM-sized window cutout with the source on top (1.7d) and on the side (1.7e).

Measurement	Peak position / ADC	Light yield / $\frac{\text{p.e.}}{\text{MeV}}$	Light yield / $\frac{\text{ph}}{\text{MeV}}$
Flat	3065.69 ± 450.48	1996.24 ± 301.74	8619.36 ± 1302.84
Vertical, Top	2110.67 ± 330.26	1356.56 ± 221.21	5857.33 ± 955.15
Vertical, Side	2196.13 ± 362.80	1413.80 ± 243.01	6104.49 ± 1049.26
Vertical, Window, Top	948.9 ± 210.69	578.39 ± 141.12	2497.35 ± 609.34
Vertical, Window, Side	975.01 ± 241.14	595.87 ± 161.52	2572.86 ± 697.41

Table 1.1: Light yield measurement results of the $50 \times 50 \times 10\text{mm}^3$ EJ-200 scintillator sample.

3 mm and 2 mm thick crystal, respectively. The SiPM-type chosen, was the already available Broadcom AFBR-S4N44P014M, with an active area of $3.72 \times 3.62 \text{ mm}^2$, a micro cell pitch of $40 \mu\text{m}$, 8334 microcells and a maximum PDE of 63 % at 420 nm coinciding with the luminescence maximum of PbWO₄. The upper limit of the expected number of triggered pixels can be calculated using the highest simulated energy loss in the Bragg-Peak region, which is approximately 40 MeV, as shown in Figure ???. Accounting for the covered active area of the SiPM by the 2 mm thick crystal gives:

$$\frac{N(E)}{N(A)} = E \cdot \frac{L \cdot \text{PDE}}{N_0 \frac{A_{cov}}{A_{SiPM}}} \quad (1.7)$$

$$\frac{N(E_{max} = 40 \text{ MeV})}{N(A)} = 40 \text{ MeV} \cdot \frac{59.7 \text{ ph/MeV} \cdot 0.63 \frac{1}{\text{ph}}}{N_0 \cdot \frac{2 \cdot 3.72 \text{ mm}^2}{3.62 \cdot 3.72 \text{ mm}^2}} \quad (1.8)$$

$$= 0.327 \quad (1.9)$$

1.6.2 SiPM for EJ-212

Since EJ-200 and EJ-212 are very similar the SiPM-type for the EJ-212 scintillators was chosen based on the measurements of EJ-200. The measured light yield for the teflon-wrapped EJ-200 scintillator with an SiPM-sized cut-out with a center positioned source is 2572.86 , as shown in Table 1.1. Due to the high light yield an SiPM, the Hamamatsu S14160-3010PS was chosen. This SiPM has an active area of $3 \times 3\text{mm}^2$, a micro cell pitch of $10 \mu\text{m}$, 89984 microcells and a maximum PDE of 18 % at 460 nm, which is close to the luminescence maximum of EJ₂₁₂ at 423 nm. The upper limit of the expected number of

triggered pixels is again calculated using the highest simulated energy loss in the Bragg-Peak region, which is approximately 20 MeV, as shown in Figure ???. Accounting for the fully covered active area of the SiPM this gives:

$$\frac{N(E)}{N_0} = E \cdot \frac{L \cdot PDE}{N_0} \quad (1.10)$$

$$\frac{N(E_{max} = 20\text{MeV})}{N(A)} = 20\text{MeV} \cdot \frac{2572.86\text{ph/MeV} \cdot 0.18\frac{1}{\text{ph}}}{N_0} \quad (1.11)$$

$$= 0.103 \quad (1.12)$$

1.7 Detector Assembly and Construction

1.8 Experimental Setup

1.9 Data Analysis

1.10 Results

1.11 Discussion

1.12 Outlook

Bibliography

- [1] JLU Giessen R. Schubert. *Personal communication*. 2024.
- [2] Hamamatsu Photonics. *R1828-01, R2059 Photomultiplier Tubes Datasheet*. Accessed: 2024-10-28. Hamamatsu Photonics K.K. 2019. URL: https://www.hamamatsu.com/content/dam/hamamatsu-photonics/sites/documents/99%5C_SALES%5C_LIBRARY/etd/R1828-01%5C_R2059%5C TPMH1259E.pdf.
- [3] *The CMS electromagnetic calorimeter project: Technical Design Report*. Technical design report. CMS. Geneva: CERN, 1997. URL: <https://cds.cern.ch/record/349375>.
- [4] Bayer AG. *Baysilone® Fluids Brochure*. Accessed: 2024-10-30. 2020. URL: <https://dcproducts.com.au/wp-content/uploads/2020/12/BayerBaysiloneFluidsBrochure.pdf>.
- [5] I. H. Malitson. “Interspecimen Comparison of the Refractive Index of Fused Silica”. In: *J. Opt. Soc. Am.* 55 (Oct. 1965). DOI: 10.1364/JOSA.55.001205.

List of Figures

1.1	Caption	4
1.3	Measurement positions of the PbWO ₄ scintillators on the PMT for the light yield measurements using a ²² Na source.	6
1.4	Example light yield measurement of the 3 mm thick PbWO ₄ -crystal number 0 in flat position on the PMT using a ²² Na source.	7
1.5	Light yield measurements of PbWO ₄ -crystals in flat and vertical positions including two window cut-out measurements using a ²² Na source.	8
1.6	Measurement positions of the EJ-200 scintillator on the PMT for the light yield measurements using a ²⁴¹ Am source.	9
1.7	Light yield measurements of the 50 × 50 × 10mm ³ EJ-200 scintillator sample. Shown are the measurements of the scintillator in a flat position with a completely open side (1.7a), in a vertical position with open side and the source on top (1.7b) and on the side (1.7c), and in a vertical position with an SiPM-sized window cutout with the source on top (1.7d) and on the side (1.7e).	10

List of Tables

1.1 Light yield measurement results of the $50 \times 50 \times 10\text{mm}^3$ EJ-200 scintillator sample.	11
--------------------------------------------------------------------------------------------------------------------	----

Selbstständigkeitserklärung

Hiermit versichere ich, die vorgelegte Thesis selbstständig und ohne unerlaubte fremde Hilfe und nur mit den Hilfen angefertigt zu haben, die ich in der Thesis angegeben habe. Alle Textstellen, die wörtlich oder sinngemäß aus veröffentlichten Schriften entnommen sind, und alle Angaben die auf mündlichen Auskünften beruhen, sind als solche kenntlich gemacht. Bei den von mir durchgeführten und in der Thesis erwähnten Untersuchungen habe ich die Grundsätze gute wissenschaftlicher Praxis, wie sie in der ‚Satzung der Justus-Liebig-Universität zur Sicherung guter wissenschaftlicher Praxis‘ niedergelegt sind, eingehalten. Entsprechend § 22 Abs. 2 der Allgemeinen Bestimmungen für modularisierte Studiengänge dulde ich eine Überprüfung der Thesis mittels Anti-Plagiatssoftware.

Datum

Unterschrift